Kuusinen N., Hovi A., Rautiainen M. (2021). Contribution of woody elements to tree level reflectance in boreal forests. Silva Fennica vol. 55 no. 5 article id 10600. https://doi.org/10.14214/sf.10600

Supplementary file S1

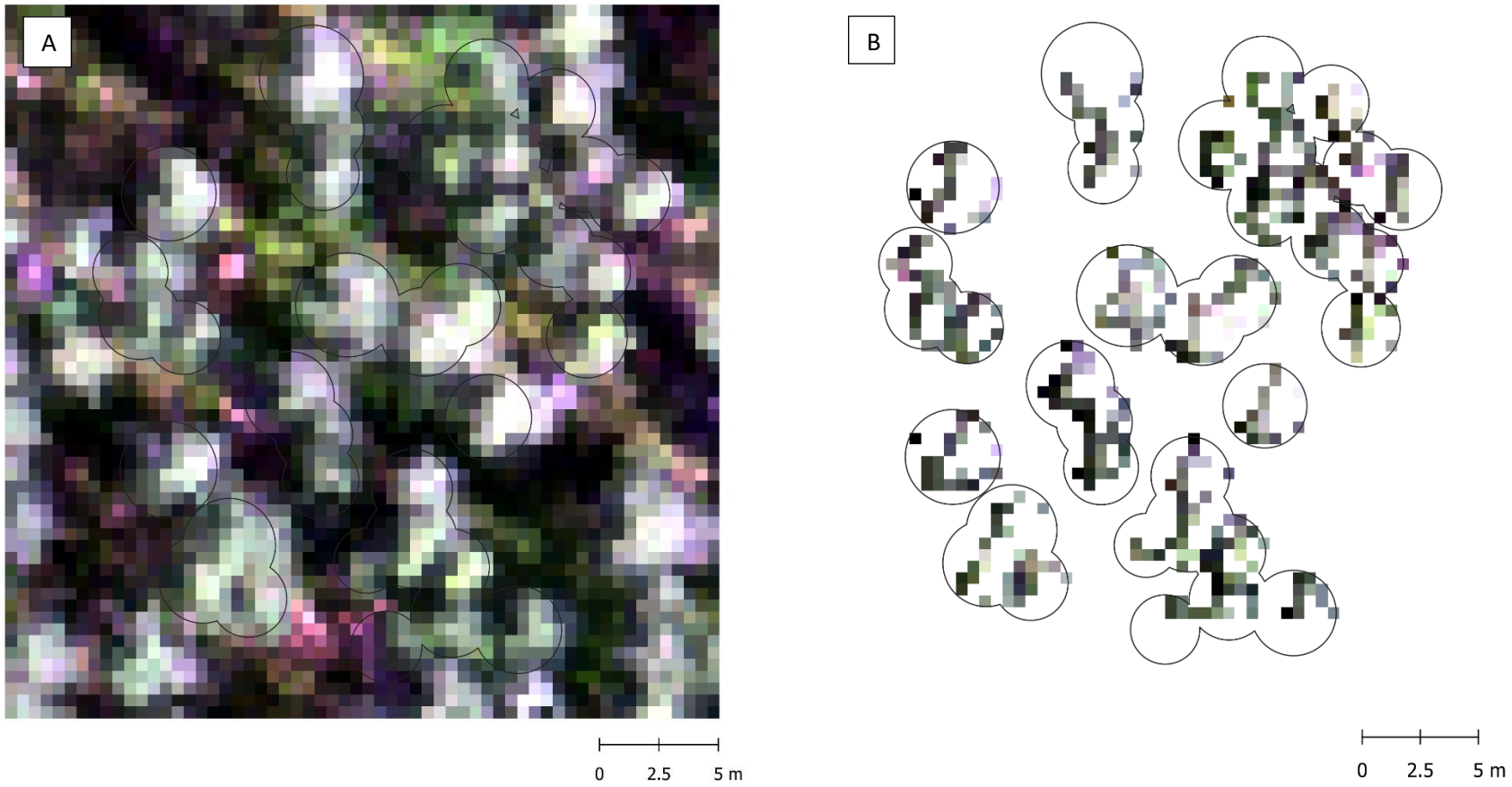

Fig. A1. An example of the pixel selection process (Section 2.2. in the article). A) Red-green-blue image of the hyperspectral airborne data from plot Pine 1 (see Table 1 in the article), as well as tree crown delineations estimated using crown width models, and B) pixels selected for analyses from plot Pine 1.

Table A1. Description of the materials and how they were used in the analyses. Further information on the analyses and citations to articles in which the measurements are explained in more detail are found from the main text (Section 2.).

Data	Description	Used in	Spectral mixture analysis
Airborne hyperspectral data	- Collected in July 2019. - Aircraft mounted CASI-1500 hyperspectral pushbroom sensor (Itres Ltd., Canada). Flight altitude 1 km. - 48 spectral bands with spectral resolution of 15 nm in 382-1052 nm. - Pixel size 0.5 × 0.5 m on the ground. - Orthorectified and radiometrically and atmospherically corrected to yield bottom-of-atmosphere hemispherical-directional reflectance factors. - Sensor view angle on the used plots less than 10 degrees.	- Spectral mixture analysis.	Normalized spectra used in Models 1-2. Original spectra used in Models 3-4.
Airborne laser scanning data	- Collected during the same flight as the hyperspectral data using Riegl LMS Q780 sensor.	- Calculation of canopy height model → pixel selection for spectral mixture analysis.	
Tree inventory	- 13 plots of 25 × 25 m from the flight area (61°50'41"N 24°17'24"E). - 4 Scots pine, 5 Norway spruce and 4 birch plots. - Location, breast height diameter (DBH), species and status measured from every tree larger than 8 cm (DBH). Height measured from two dominant trees per plot.	- Information of tree species, location and status → pixel selection for spectral mixture analysis. - Calculation of average forest variables in plots.	
Crown width models	Pine (m): 1.1852+0.1159DBH (n=51, r^2=0.74, RMSE=0.048) (DBH in cm) Spruce (m): 1.4035+0.1003DBH (n=65, r^2=0.79, RMSE=0.045) (DBH in cm) Birch (m): 1.695+0.126DBH (n=45, r^2=0.50, RMSE=0.053) (DBH in cm)	- Pixel selection for spectral mixture analysis.	
Hemispherical photographs	- 21 hemispherical photographs per plot taken in diffuse sky conditions. - Nikon D5000 digital camera with a fisheye lens. - Measuring height 1.5 m.	Estimation of effective plant area index (PAI_{eff}), diffuse interceptance, gap fraction in the solar direction (t_{0d}) and within-crown gap fraction in the sensor direction (t_{0s}) for each plot.	
Needle and leaf spectra*	- 3 trees of each tree species were sampled from the study area. - Reflectance and transmittance spectra were measured using an integrating sphere attached to an ASD FieldSpec4 spectrometer (350-2500 nm). - Needles and leaves sampled from top-of-canopy (sun-exposed), bottom-of-canopy (shaded), current-year and one-year-old needles (pine and spruce). - Both sides of each leaf or needle sample measured. - Needle/leaf albedos calculated as sums of reflectance and transmittance.	- Band selection (foliage + bark spectra) → spectral mixture analysis.	Normalized spectra used in Models 1-2. Original spectra used in Models 3-4.
Forest floor spectra*	- Measured in diffuse sky conditions, from 15 points along an 11-m-long transect located in the center of each plot. - ASD FieldSpec4 spectrometer (350-2500 nm). - Nadir view measurements at approximately 1.3 m height. - White reference measured at every 3rd measurement point.	- Multiplied by gap fraction estimates (obtained from hemispherical photographs) and subtracted from reflectance of the airborne hyperspectral data to remove the direct forest floor contribution.	Used in Models 2 and 4 only.
Bark spectra*	- 2 Scots pine, 2 Norway spruce and 2 silver birch trees. - Specim IQ hyperspectral camera (400-1000 nm). - Bark spectra measured from 10 heights along each stem in a laboratory. - Nadir view measurements used in this study. - Collected from Vantaa, southern Finland (i.e., different study area than in the other measurements).	- Band selection (foliage + bark spectra) → spectral mixture analysis.	Normalized spectra used in Models 1-2. Original spectra used in Models 3-4.

* Spectra resampled to correspond to the bands of the airborne hyperspectral data.

Acquisition and processing of hemispherical photographs

A total of 21 hemispherical photographs per plot were taken, from a 10-m grid covering an area of 30 x 30 m (i.e., 4×4=16 photographs) around the center of the plot, and additionally from center of the plot and from spots located 5 m to each cardinal direction from the center (i.e., 5 photographs). We used a Nikon D5000 digital camera with a geometrically calibrated (i.e., lens distortion corrected) Sigma 4.5 mm 1:2.8 DC HSM Circular Fisheye lens. The height of the camera from the ground was 1.5 m, and the photographs were taken in diffuse illumination (early in the morning, late in the evening, or overcast sky conditions during daytime). Highest quality 8-bit JPEG format was used (ISO-200, aperture size fixed at *f*/5, lens focused to infinity). The exposure time for each photograph was adjusted to prevailing light conditions, by observing the image histogram on the camera screen. Two additional photographs, with exposure time halved and doubled from the original exposure time, were also taken. In post-processing we chose the photograph in which the pixel values in the blue channel filled the dynamic range of eight bits as well as possible, but the histogram was not saturated.

The photographs were thresholded into binary images, by applying the algorithm by Nobis and Hunziker (2005) to the blue channel. Additionally, to paint the small within-crown gaps in black and thus enabling computation of between-crown gap fraction, we performed morphological closing and opening operations for the binarized images as described in Korhonen and Heikkinen (2009). A disk-shaped structuring element with radius of 10 pixels was used in the morphological operations (see Korhonen and Heikkinen 2009 for explanation of these parameters). Gap fraction values (total and between-crown gaps) were then computed for five concentric zenith rings with median zenith angles of 10.7°, 23.7°, 38.1°, 52.8°, and 66.6°. Within-crown gap fraction was obtained by subtracting the between-crown gap fraction from total gap fraction. Two effective plant area index (PAI_{eff}) estimates were calculated: one using total gap fraction, and the other using only within-crown gap fraction. The equation for PAI_{eff} was the same as used by the LAI-2200 instrument (LI-COR 2012):

$$\mathrm{PAI}_{eff} = 2\sum_{i=1}^{5} K_i W_i \qquad \text{(Eq. A1)}$$

where K_i=-ln$t_0(\theta_i)$cosθ_i, and W_i=sin$\theta_i d\theta_i$ (sum of W_i equals 1), and $t_0(\theta_i)$ is the gap fraction (total or within-crown) in the *i*th zenith ring. We denote PAI_{eff} calculated using total gap fraction as 'PAI_{eff}' and that calculated using within-crown gap fraction as 'crown PAI_{eff}' (effective plant area per vertical crown projection area). Finally, diffuse interceptance (i_D) was calculated using total gap fraction, following the LAI-2200 user manual (LI-COR 2012) as

$$i_D = 1 - 2\sum_{i=1}^{5} t_0\left(\theta_i\right) W'_i \qquad \text{(Eq. A2)}$$

where W'_i=sin$\theta_i$cos$\theta_i d\theta_i$ (sum of W'_i equals 0.5).

Measurement and processing of leaf and needle spectra

Leaf and needle directional-hemispherical reflectance and transmittance spectra at wavelengths of 350–2500 nm were measured for samples taken from top-of-canopy (sun-exposed canopy position) and bottom-of-canopy (shaded canopy position) needles or leaves. For coniferous needles, two age cohorts, current year (c_0) and one-year-old (c_1) needles, were sampled. The number of samples in each tree was three per each canopy position and per each age cohort, i.e., for a coniferous tree there were 12 samples and for a broadleaved tree six samples. Only healthy foliage was measured. The leaf and needle albedo spectra were calculated as sums of reflectance and transmittance.

The measurements were conducted with an ASD RTS-3ZC integrating sphere attached to an ASD FieldSpec4 spectrometer (ser. nr. 18641). During the measurement, both needles and leaves were attached to 0.3-mm-thick needle carriers (Fig. 1 in Hovi et al. 2020). When attaching the needles, spacing of 0.5–1× needle width was used. For all leaf and needle samples, reflectance and transmittance of both sides of the sample were measured. Additionally, white reference measurements for reflectance and transmittance were taken. A Spectralon panel with 99% nominal reflectance was used as white reference. Stray light in the reflectance measurement configuration was also measured, using a photon trap. The configurations of the sample, white reference, and photon trap in each type of measurement have been described in detail in Hovi et al. (2020). The raw data were processed into leaf (or needle) reflectance (R_L) and transmittance (T_L) as

$$R_L = \frac{q_R}{q_{ref,R}} \frac{1}{1-P_{gap,R}} R_{ref}\text{, and} \qquad \text{(Eq. A3)}$$

$$T_L = \left(\frac{q_T}{q_{ref,T}} - P_{gap,T} \right) \frac{1}{1-P_{gap,T}} R_{ref}\text{,} \qquad \text{(Eq. A4)}$$

where q_R and q_T are the measured raw radiation signals (digital numbers) from the reflectance and transmittance measurements, $q_{ref,R}$ and $q_{ref,T}$ are the measured raw radiation signals from the white reference measurements for reflectance and transmittance, respectively, R_{ref} is the reflectance of the white reference panel, and $P_{gap,R}$ and $P_{gap,T}$ are gap fractions in the sample (zero for leaves of broadleaved species). Stray light was subtracted from q_R and $q_{ref,R}$ before calculations. The gap fractions were calculated from grayscale images obtained by scanning the carriers with needle samples, using a digital film scanner (Epson Perfection V550). The scan resolution was 800 dpi. A gray level threshold (200 for pine, 229 for spruce) was applied to an area of the scanned image that represented the portion of sample that was illuminated by the light beam in the measurement. The procedure for determining gap fractions has been described in detail in Hovi et al. (2020). The optimal gray level threshold values were found by comparing gap fractions calculated from the scanned images to reference gap fractions in a subset of needle samples (12 samples per species). The reference gap fraction was obtained by painting the needles in black, which ensured that the radiation signal in the transmittance measurement was only caused by the transmission of light beam through between-needle gaps, i.e., the signal quantified the gap fraction directly. Finally, to correct for a small transmittance bias inherent to the ASD RTS-3ZC integrating sphere (Hovi et al. 2020), we applied an empirical correction (adjustment of transmittance values by 5.5% downwards in relative terms) to both leaf and needle transmittance values. The correction ensured that absorption in the near-infrared was always positive.

References

Hovi A, Mõttus M, Juola J, Manoocheri F, Ikonen E, Rautiainen M (2020). Evaluating the performance of a double integrating sphere in measurement of reflectance, transmittance, and albedo of coniferous needles. Silva Fenn 54, 10270. https://doi.org/10.14214/sf.10270

Korhonen L, Heikkinen J (2009) Automated analysis of in situ canopy images for the estimation of forest canopy cover. For Sci 55: 323–334. https://doi.org/10.1093/forestscience/55.4.323

LI-COR 2012. LAI-2200 plant canopy analyzer instruction manual. LI-COR, Inc., publication number 984-10633 rev 2. https://www.licor.com/documents/6n3conpja6uj9aq1ruyn

Nobis M, Hunziker U (2005) Automatic thresholding for hemispherical canopy-photographs based on edge detection. Agr Forest Meteorol 128: 243-250. https://doi.org/10.1016/j.agrformet.2004.10.002